LOAD SHARING AND DAMAGE REDUNDANCY OF RIBBED WOODEN ELEMENTS

LASTVERTEILUNG UND SCHÄDIGUNGSREDUNDANZ VON HOLZ-RIPPENELEMENTEN

Simon Aicher[1], Nikola Zisi[1], Iztok Sustersic[2]

[1] *Materials Testing Institute (MPA), University of Stuttgart, Otto-Graf-Institute*

[2] *InnoRenew CoE, Izola, Slovenia*

SUMMARY

Monolithic full cross-sections represent independent of the respectively used material – concrete, steel or wood – resource inefficient, technically-economically insufficient solutions. This is especially true for elements subjected to bending. Intelligent construction elements such as ribbed plates or box-beams enable equal mechanical performance at substantially reduced material consumption. This is essential in view of the increasing importance of the sustainability of building products and construction methods.

The paper reports on the load carrying and damage behaviour of wooden ribbed elements made of cross-laminated timber (CLT) sheeting and solid wood ribs, which were investigated profoundly in a recent European WoodWisdom research project *HCLTP*. From mechanical viewpoint the load redistribution behaviour and the resulting damage tolerant, quasi-hardening global load-deflection behaviour, which is influenced essentially by the stiffness differences between the ribs, is of prime interest.

The global stiffness reduction as well as the different strain and stress distributions in the cross-section due to progressive damage of the ribs is mirrored by finite element calculations. Finally, in view of the revision of the European timber design code Eurocode 5 (EC5) recommendations are given for a system factor of glued wooden ribbed elements.

ZUSAMMENFASSUNG

Monolithische Vollquerschnitte repräsentieren insbesondere bei biegebeanspruchten Bauteilen unabhängig vom jeweilig verwendeten Material – Beton, Stahl oder Holz – ressourcenineffiziente, technisch-wirtschaftlich ungenügende

Lösungen. Intelligente Bauelemente wie Rippenplatten oder Kastenträger ermöglichen bei erheblicher Verminderung des Materialeinsatzes gleichwertige mechanische Leistungen, was im Hinblick die zunehmend bedeutsamere Nachhaltigkeitsrelevanz von Bauprodukten und Bauweisen essentiell ist.

Im vorliegenden Aufsatz wird über das Trag- und Schädigungsverhalten von Holz-Rippenelementen aus Brettsperrholz (BSP)-Beplankung und Vollholzrippen berichtet, die in dem europäischen WoodWisdom-Forschungsvorhaben *HCLTP* eingehend untersucht wurden. Mechanisch steht hierbei das Lastumlagerungsverhalten und das hieraus resultierende schädigungstolerante, quasi verfestigende globale Last-Verformungsverhalten im Vordergrund, das durch Steifigkeitsunterschiede zwischen den Rippen wesentlich beeinflusst wird.

Die globale Steifigkeitsreduktion sowie die sehr unterschiedlichen Dehnungs- und Spannungsverteilungen im Querschnitt infolge progressiver Schädigung in den Rippen werden durch Finite Element Berechnungen abgebildet. Abschließend werden mit Blick auf die Neufassung der europäischen Holzbaunorm Eurocode 5 (EC 5) Empfehlungen für einen Systemfaktor von verklebten Holzrippenelementen gegeben.

KEYWORDS: Ribbed elements, CLT sheeting, solid wood ribs, load redistribution, damage tolerance, system factor, EC5

1. INTRODUCTION

The use of timber in present day building construction is experiencing an unprecedented increase due to its well-known technical advantages, as well as due to its indisputable assets in enabling sustainable construction works. Sustainability and reduction of CO_2 emissions have become the all dominating, lead aspects in the construction industry as the devastating footprint of the industry, with about 40% of the world´s total CO_2 emissions, has become a public concern.

Timber construction is nowadays regarded as a major key to address and resolve the global warming hazzard. In this context the construction of medium and high rise timber buildings is progressing with immense speed, hereby relaying extensively on massive timber products, such as cross-laminated timber (CLT), a so-called mass wood product with versatile use in walls, floors and roofs. CLT, built up from cross-wise layered and adhesively bonded boards represents a quasi homogeneous product similar to concrete, however with significantly higher, tensile

capacity at lower density. However, analogous to a reinforced concrete slab, all the material in the centre part of the cross-section is marginally used, especially in bending, and is therefore in technical, economical and sustainability sense wasted. As wood is becoming a major material source in worldwide construction industry, the material saving issues represent a primary aspect irrespective of the undisputed superiority of the wood as a sustainable material in general. In order to address this issue, already some very successful attempts were/are made to use ribbed plates, as a highly economical and technically equivalent alternative [e.g. 1, 2].

In this article an interesting aspect of ribbed wooden elements being their articulate load redistribution possibility resulting from stiffness and strength variability of the components and the hereon based load capacity redundancy are discussed. A proposal for an increased system factor in the new Eurocode 5 is made.

2. EXPERIMENTAL RIBBED ELEMENTS CAMPAIGN

The experimental and computational results presented in this paper were obtained within the frame of a recent European Wood Wisdom research project HCLTP (Hybrid Cross Laminated Timber Plates). For detailed information on the project and respective results, see [3-5]. The research dealt mainly with ribbed elements and their technical and economical advantages to monolithic slab constructions.

Within this thematic area investigations on the relative advantage of two significantly different production methods for ribbed plates were performed, being i) the conventional approach by bonding a completed CLT plate to ribs and ii) manufacturing the whole ribbed compound in a single step bonding/cramping process. Related findings have been published previously and are not discussed here. The advantages of ribbed vs. monolithic plates with regard to wood material and hence economic savings are discussed and quantified in [6].

This paper addresses exclusively the aspect of load sharing in the context of damage progression redundancy of ribbed wooden elements, e.g. [7]. The reported characteristic behaviour of ribbed elements has been witnessed in the mentioned project as well as in many previous tests and evaluations at MPA University of Stuttgart. Numerous respective tests have been performed within the frame of technical approvals, compliance decisions by state building authorities for individual cases and especially at qualification tests for acquiring a bonding certificate type D for ribbed structures according to DIN 1052-10 [8].

3. ELEMENT BUILD-UP AND TESTING

Fig. 1 shows the cross-sectional build-up of the considered element configuration with a total length of 4 m. It consisted of an industrially manufactured 3-layer CLT-plate (laminations of grade C24 with thickness of 40 mm) that was bonded to three parallel arranged solid wood (spruce) boards, hereinafter called ribs, each with a cross-section of 40 x 30 mm. Initially, the boards were graded visually according to DIN 4074-1 [9] in the class S13 conforming to strength class C30 according to EN 1912 [10]. Subsequently the boards were additionally characterized by weighing and by determining the modulus of elasticity (MOE) parallel to fiber by analysing the longitudinal vibration frequencies induced with the impulse excitation technique (device GrindoSonic MK5). As summarized in Table 1, the density and MOE of all rib boards were significantly higher as of the plate element. The rib labelled as 1 contained a finger joint located in the constant moment region.

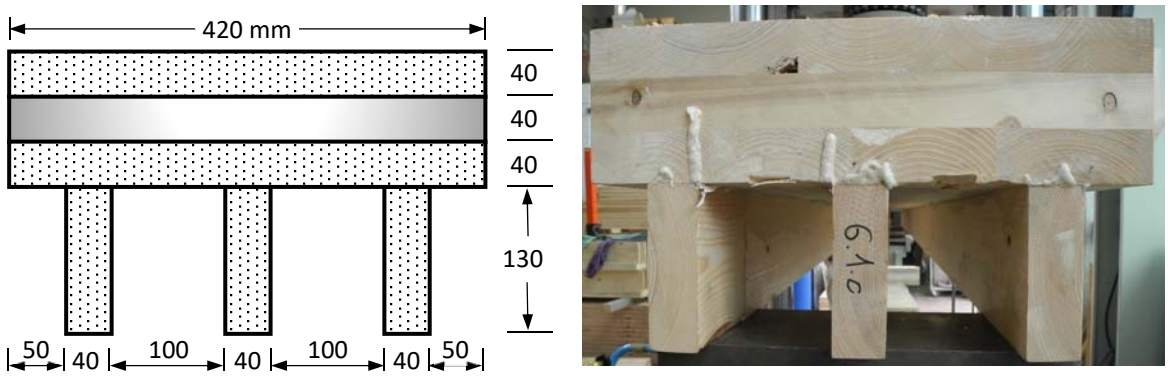

a) b)

Fig. 1: Cross-sectional build-up of investigated ribbed element a) dimensions b) view of glued composite

Table 1: Density, modulus of elasticity and existence of finger joints in constant moment area of the ribbed element 6.1a

characteristics	unit	ribs		
		1	2	3
density	[kg/m^3]	550	502	512
MOE, E_0	[GPa]	20,7	15,3	16,9
finger joint	-	yes	no	no

The ribs were bonded to the CLT-plate in a hydraulic press (pressure ~ 0,8 N/mm^2) by means of a moisture curing one-component polyurethane adhe-

sive qualified for structural bonding as type EN 15425 I 90 GP 0,3 [11]. The spacing of the ribs was intentionally very narrow as the specific investigations aimed to provide a ribbed alternative to a monolithic 5-layer CLT-plate, while achieving a 35% lower material consumption. Due to the very narrow spacing of the ribs (clear width: 100 mm), no reduction of the effective width of the slab had to be considered. In a global view, the element represents three T-shaped beams aligned and rigidly jointed in parallel characterized by a roughly equal compressive flange and ribs of different stiffness and strength.

The element was tested in a 4-point bending set-up with a span of 3,78 m. The two concentrated loads (F/2), applied uniformly in the transversal direction, were placed at the third points. The element was supported at the bottom of the ribs without any additional stiffening. The loading was applied through a distribution beam attached to the piston of a servo-hydraulic test machine. The advance of the piston was displacement controlled, with a constant speed of 6,5 mm/min. Fig. 2a shows a view of the test set-up.

The applied piston force F during the testing was obtained directly from the machine. The global mid-span deflection of the element was measured with two displacement transducers placed at mid-span near the element edges. Linear strain gauges were installed in the constant moment area to monitor the damage evolution in more detailed manner. They were placed at the narrow bending tension edge of each rib as well as at the bottom and top surfaces of the CLT plate. In the placement of the strain gauges care had been taken to avoid large fibre deviations and knots and yet being as close to the mid-span as possible. Due to a knot near the mid-span at rib 1, two strain gauges were installed, one on each side of the knot (see Fig. 2b).

The test was conducted at room temperature (≈ 20°C) and uncontrolled relative air humidity. The moisture content of the ribs and the CLT-plate at the time of testing was on average about 9% for both component types.

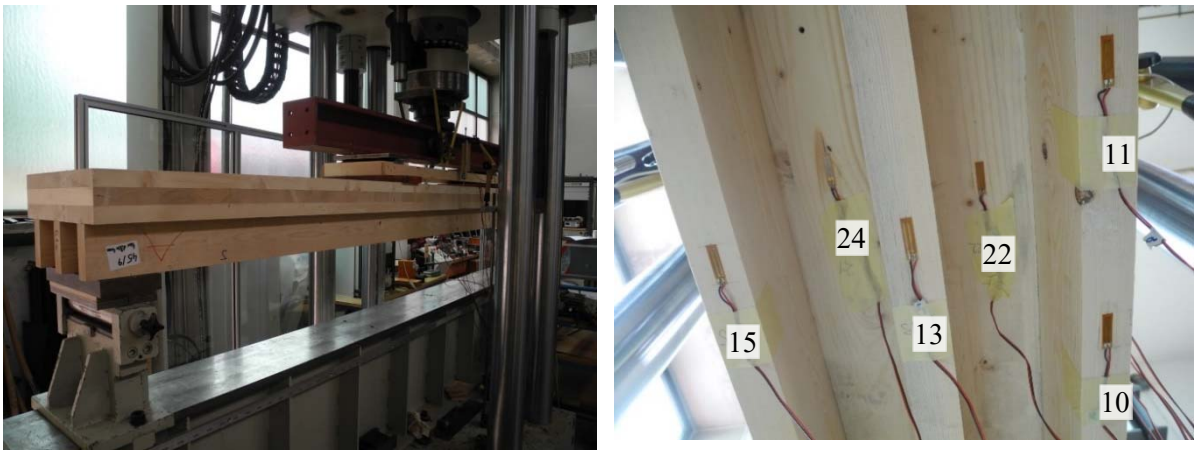

a) b)

Fig. 2: Experimental details of investigated ribbed element, a) realized test set-up, b) strain gauges at bending tensile edge of ribs and CLT plate

4. LOAD-DISPLACEMENT, STRAIN AND DAMAGE EVOLUTION

The exemplary reported measured global load displacement as well as the results of the local strain measurements and the damage observations, although related explicitly to the test configuration of test series 6.1 [4] and its three repetitive specimens here (No. 6.1a), hold in general sense true for all investigated loading and comparable build-up.

The progressive damage evolution is depicted in two overview graphs shown in Figs. 3 and 4. Fig. 3 shows the relationship of applied total force or maximum bending moment vs. average mid-span deflection until ultimate failure (here defined as damage state of the element with no load recovery beyond 50% of ultimate load in the displacement driven test). The graph shows several distinct, strong or lesser-accentuated load drops d_1 to d_5 following the linear stiffness range. The reasons for the stiffness discontinuities lay in partial or complete failures of the ribs as recorded by the strain measurements (depicted in Fig. 4) and visual observation as well.

Following in the explanation of the progressive damage it is referred to both Figs. 3 and 4 at the same time. The very small first global load drop (2% vs. prior load), which occurred at a total load of $F_{max,1}$ = 101,5 kN, is related to damage occurrence d_1. During the test, no exact visual allocation of the audible crack noise could be made, however a sudden longitudinal strain drop of about 8% could be noticed at strain gauge 13 at the narrow bending tension edge of the center rib 2.

In a very close follow-up of damage d_1, a further minor global load drop due to damage d_2 occurred. The latter damage could be related by the strain recordings and further visually (not shown here due to page limitations) to a further damage progression in the pre-damaged rib 2 and a damage in rib 1. Then, after a load increase of about 12%, vs. $F_{max,1}$ a further very small load drop in the global load deflection line occurred then attributed to damage d_3 occurring exclusively in rib 1, as evident from the strain graph in Fig. 4.

In the following a linear load increase up to damage stage d_4 associated with load $F_{max,4}$ =124,8 kN, i.e. well 20% above the first damage occurrence d_1 was encountered. At d_4 a significant abrupt global load drop of about 15% occurred. It should be mentioned that the maximum global stiffness reduction between damage states d_1 and d_4 was about 7%, so rather low. The physical reason for damage d_4 was the complete failure of the pre-damaged rib 2, what is apparent from the strain recordings shown in Fig. 4. Further, damage progression occurred in rib 1, causing rupture of the strain gauge 11.

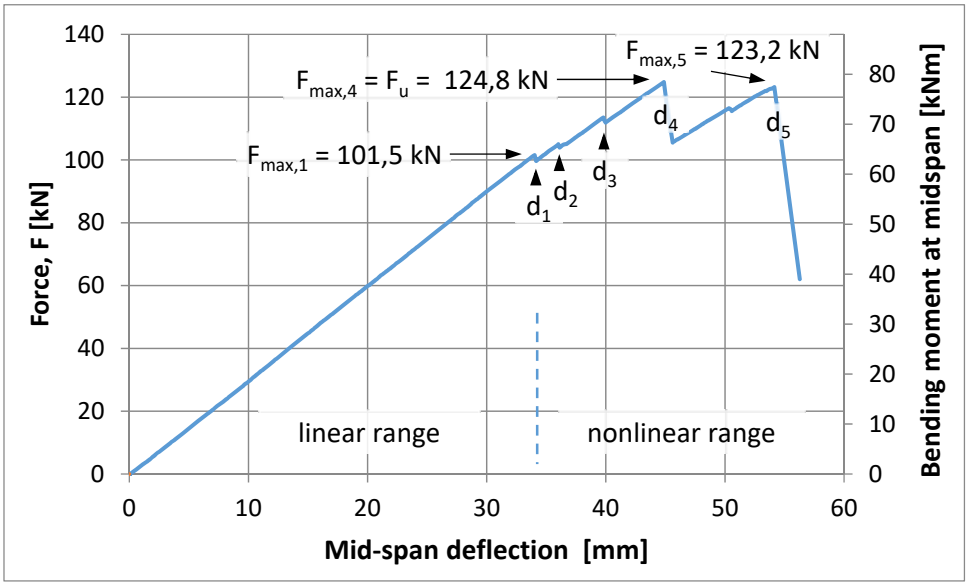

Fig. 3: Global force/bending moment vs mid-span deflection of specimen 6.1a with marked damage occurrences d_i

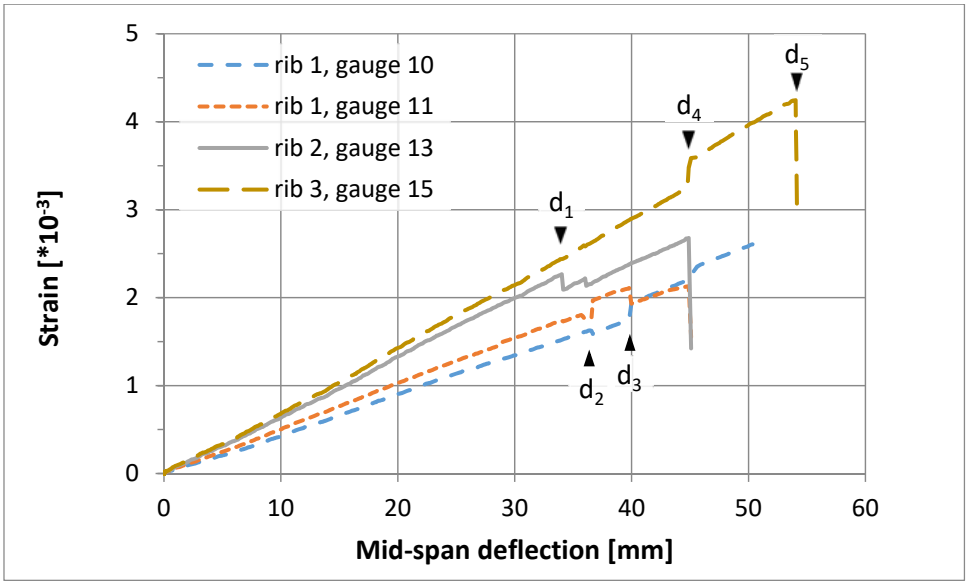

Fig. 4: Longitudinal rib strain vs. mid-span deflection curves with marked damage events

In an immediate consequence of the failure of rib 2 a sudden strain increase and hence load redistribution to ribs 1 (gauge 10) and 3 (gauge 15) can be observed from the respective strain curves in Fig. 4. Especially the abrupt stiffness response of the so far undamaged rib 3 corresponds entirely to the virgin stiffness stage of that rib, just shifted by the increased load uptake. In a follow-up of damage stage d_4, a further load recovery at a markedly reduced global secant stiffness (~24%) was encountered. Ultimate failure (d_5) occurred at $F_{max,5}$=123,2 kN related to a collapse of rib 1 bound to a finger joint fracture (see Fig. 5).

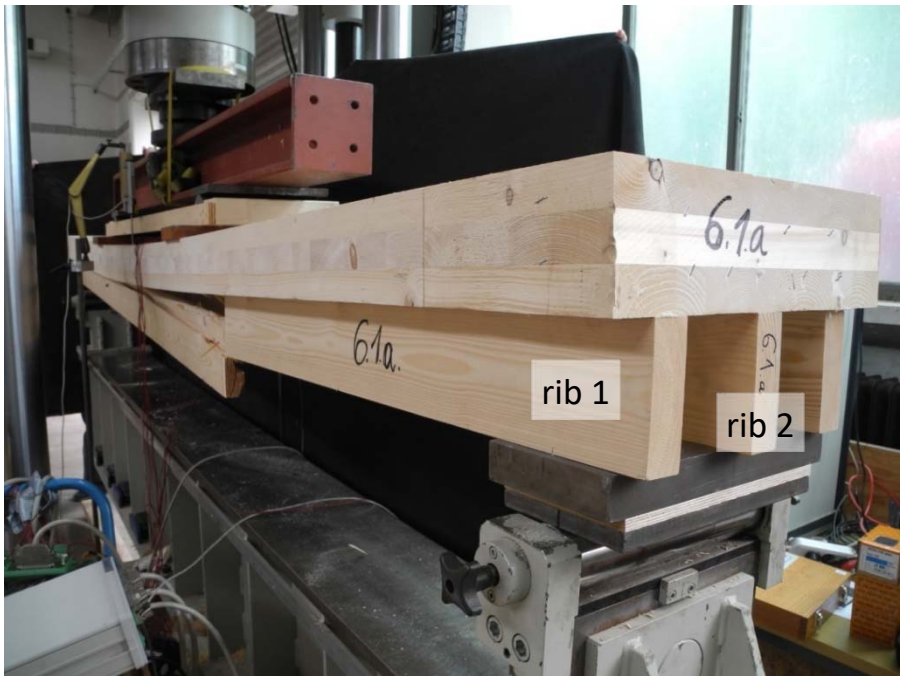

Fig. 5: View of element 6.1a at ultimate failure d_5 induced by a finger joint fracture in rib 1

5. ANALYSIS OF ELEMENT AT DIFFERENT DAMAGE STATES

The computational approach reported here briefly aimed at an engineered understanding and quantification of the non-linear strain-stress-relationships associated to the progressive damage.

5.1 ANALYTICAL CALCULATIONS

The (semi-) analytical calculation of the build-up to verify the FEM-results in the initial elastic range was performed twofold: i) rigid compound theory assuming no shear lag effect of the CLT cross-layer and ii) by the so-called shear analogy method as stated in DIN EN 1995-1-1/NA [12] for compounds with not negligible shear deformations in distinct layers of the composite. Modulus of elasticity (MOE) parallel to fiber of the outer C24 CLT-laminations was assumed as $E_{0,mean,z} = 11000$ N/mm^2 and MOE of the inner cross-layer perpendicular to the outer layers $E_{0,mean,z}$ was set to zero due to un-bonded narrow edges of boards in the cross-layer. Rolling shear modulus of the cross-layer in z-direction was taken as $G_{R,mean,z} = 0{,}1 \cdot G_{mean,z}$, with $G_{mean,z} = 670$ N/mm^2 according to EN 338 [13].

Figs. 6a, b give the results according to shear analogy method which differ for the regarded build-up only marginally (< 1%) from the computation assuming a rigid compound with $EI_{glob,rigid} = 3{,}491 \cdot 10^{12}$ Nmm^2. In order to show the agreement of

the analytical method with the FEM-calculation it has to be mentioned that the depicted stress distributions are based on rib MOEs reduced by 10% versus the frequency based values specified in Table 1 (as a result of FEM-model calibration with the experimental stiffness, see below).

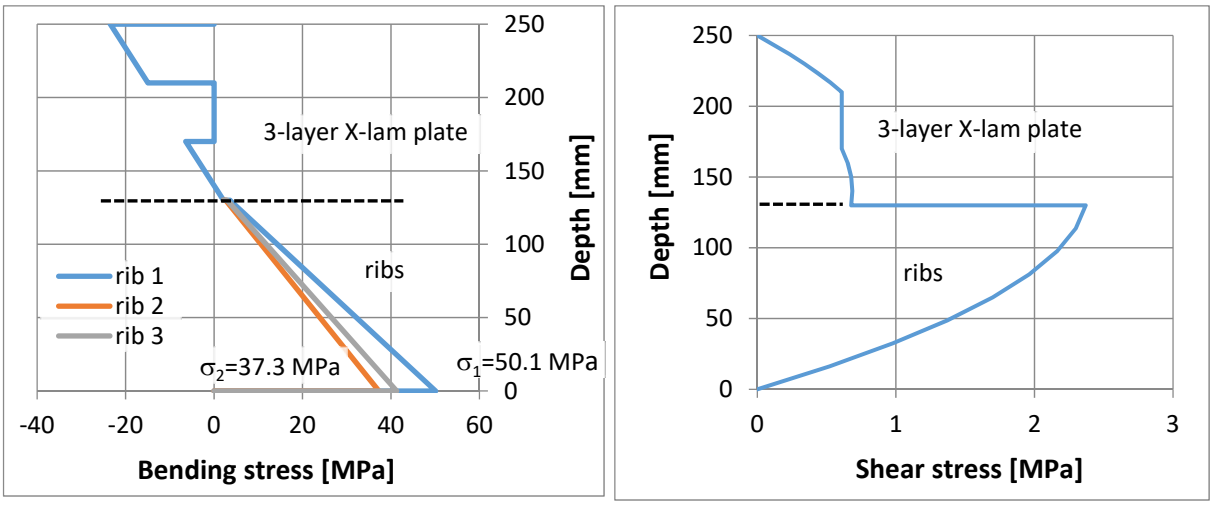

a) b)

Fig. 6: Stress distributions along cross-sectional depth of regarded build-up calculated by shear analogy method (load $F_{max,1}$ = 101,5 kN) a) bending stress b) shear stress

5.2 FINITE ELEMENT METHOD CALCULATIONS

An iterative method described below was used to model the damage evolution. It is important to note that the obtained partly pronounced nonlinear strain and stress distributions result exclusively from element state changes (alive or dead) and not from nonlinear constitutive relationships, i.e. the undamaged material remains in elastic state. The structure was modelled using the FEM-code ANSYS Rev.17.1, with 8-node volume elements (SOLID185) utilizing the symmetry condition at mid-span. The number of element divisions along cross-sectional depth was 25. The constitutive law was chosen as rhombic anisotropic using the stiffness quantities as specified in 5.1 and Table 1. For the C24 laminations of the CLT the MOEs in both directions x,y perpendicular to fiber direction were assumed as $E_{90,mean,x/y} = 370$ N/mm^2. The stiffness quantities of the ribs that were not stated in Table 1 were assumed according to the stiffness ratios specified in EN 338 [13], i.e.

$E_{90,mean,x/y\ (1\text{-}3)} = E_{0,mean,z(1\text{-}3)} / 30$ and

$G_{mean,x/y\ (1\text{-}3)} = E_{0,mean,z(1\text{-}3)} / 16{,}4$

Poisson ratios were taken as $\nu_{xz} = \nu_{yz} = 0{,}015$ and $\nu_{xy} = 0{,}4$.

5.2.1 Methodology for global stiffness adjustment

In a first step the elastic behavior of the structure in the undamaged state up to the pre-peak damage d_1 at $F_{max,1}$ was tuned to match the measured global stiffness. To do so, the measured MOEs of the ribs were appropriately scaled, whereas the stiffness properties of the CLT slab remained as specified. (Note: this approach is justified by two arguments: i) the CLT stiffness properties represent a combined action of multiple boards delivering a smeared average contribution of this component to the global stiffness response, and ii) the strains measured at the top and bottom surfaces of the CLT plate were in line with the chosen assumption.

An ideal agreement of the FEM-calculated bending stiffness and the experimentally obtained value from the performed test was achieved by reducing the measured MOEs of all the ribs given in Table 1 by 10%. The coinciding slope of the calculated and measured stiffness (here force/bending moment vs. mid-span deflection) can be seen in Fig. 7a. The empiric and the calculated bending stiffness in the elastic undamaged range 0-d_1 amounting to $EI_{glob,FEM,0\text{-}1} = 2{,}924 \cdot 10^{12}$ Nmm^2 is about 16% lower as compared to the analytically derived value based on the nominal CLT and rib stiffnesses.

The subsequent global stiffness reductions induced by the successive damage occurrences d_1 to d_4 were modelled in smeared integrative manner as one process with a constant global stiffness between damage d_1 and d_4 (of course the individual stiffness reductions from d_1 to d_2 to d_3 to d_4 could be modelled alike). The empiric and FEM approximated global stiffness between damage points d_1 and d_4 is $EI_{glob,FEM,1\text{-}4} = 2{,}261 \cdot 10^{12}$ N/mm^2 and hereby 23% lower than the effective initial stiffness. The reduction of the secant stiffness $EI_{glob,FEM,0\text{-}4} = 2{,}718 \cdot 10^{12}$ N/mm^2 vs. the undamaged state is significantly smaller in the order of 7%.

The modeling approach to obtain the reduced stiffnesses $EI_{glob,FEM,0\text{-}4/1\text{-}4}$ consisted in the removal of elements from the FE model at the locations where the visible and measurable damage occurred. This procedure is highlighted in Fig. 7b for the severely damaged structure state between damages d_4 and d_5.

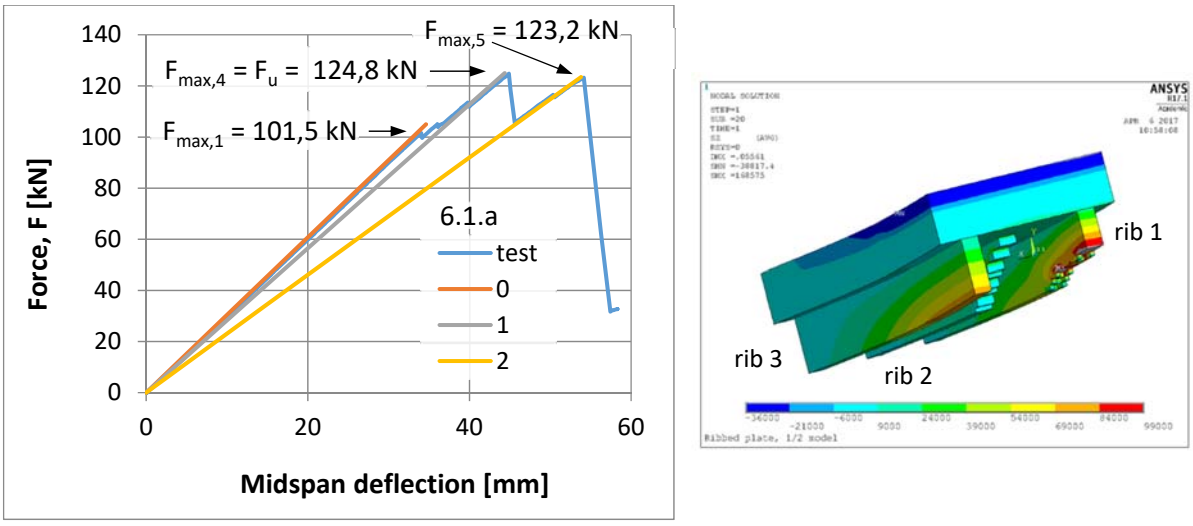

a) b)

Fig. 7: FEM approximation of test results a) global stiffnesses at different damage states b) visualization of FEM model with partially damaged ribs(damage state d_5)

The derivation of $EI_{glob,FEM,0\text{-}5}$ and hereby $EI_{glob,FEM,4\text{-}5}$ was done as in the previous damage states. Although the stiffness $EI_{glob,FEM,4\text{-}5}$ is only slightly smaller (4%) as compared to the previous damage step $EI_{glob,FEM,3\text{-}4}$ the global secant stiffness reduction before damage d_5 now amounted to 24%.

Finally, both the empirically obtained global stiffness and the coinciding FEM model stiffness can be evaluated for the stiffness reduction between first damage d_1 and last damage d_5 prior to ultimate failure. The stiffness $EI_{glob,FEM,1\text{-}5} = 1{,}136 \cdot 10^{12}$ N/mm^2 is 60% lower than the effective elastic stiffness but, and very important, the progressive damage presents globally a hardening and finally a quasi-ductile, damage tolerant behavior.

5.2.2 Strains and bending stresses

The consequences of the localized damages on the longitudinal strains and associated bending stresses in the (un)damaged ribs are revealed in Figs. 8a-f. They depict the longitudinal strains and the bending stresses at (immediately prior) to the three articulate loading and damage states d_1, d_4 and d_5. In each graph, the strains or the complementary stresses are given for three sections along the depth of the element each of them located at mid-width of the ribs 1, 2 and 3, respectively. Figs. 8a, b depict the strain and stress distribution prior to damage d_1 at $F_{max,1}$=101,5 kN. Figs. 8c, d give the strain and stress distributions prior to damage d_4 at the ultimate load F_u=$F_{max,4}$=124,8 kN, while Figs. 8e, f give the strain

and stress distributions at complete failure of the specimen, i.e. at damage d_5 and force $F_{max,5}$=123,2 kN. The graphs reveal that strains and stresses in the individual ribs, bound to their respective stiffness and strength properties, are significantly different, finally enabling the encountered damage tolerant global element behavior. A thorough discussion of the sensible strain-stress distributions is subject of a follow-up publication.

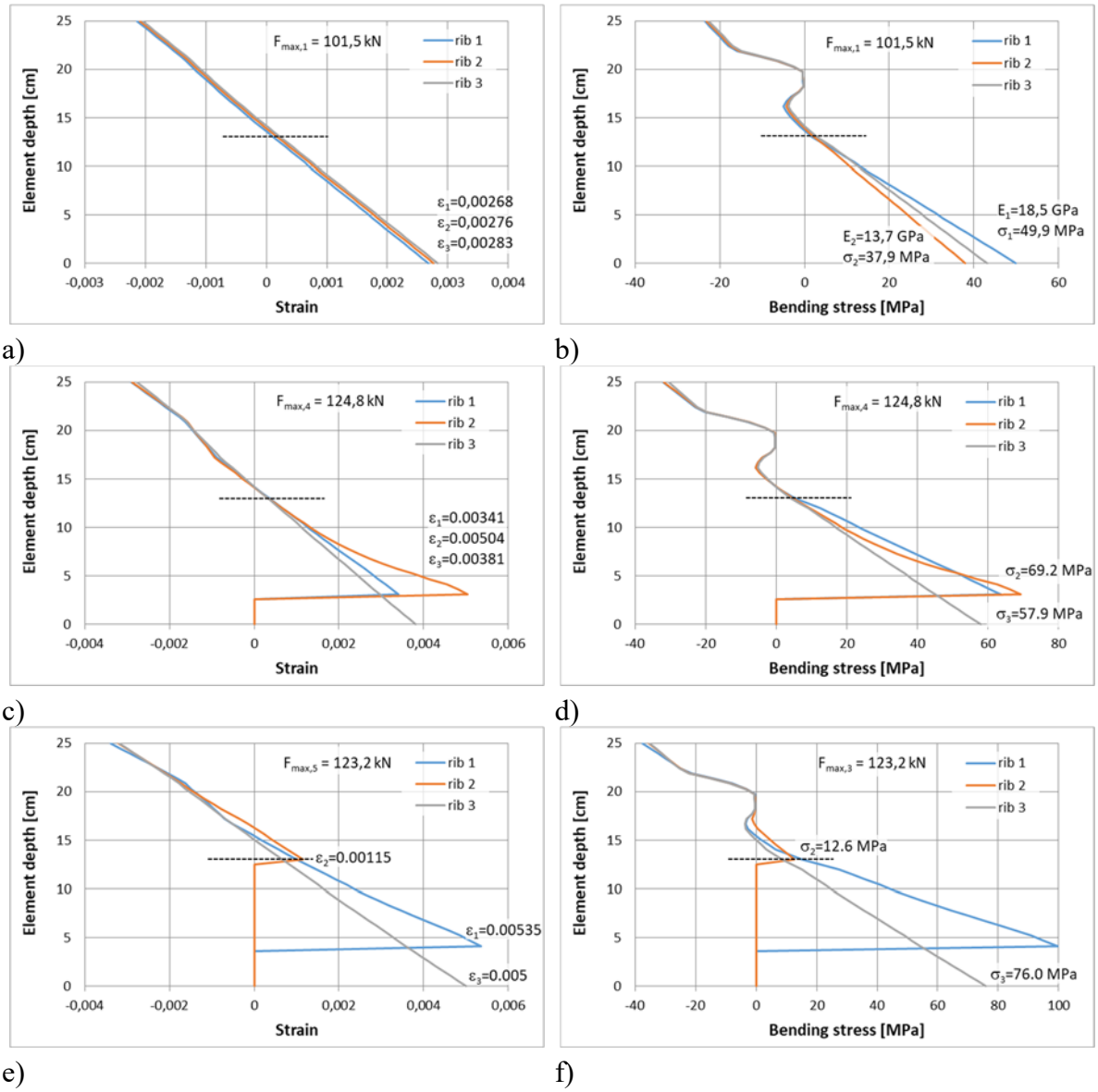

Fig. 8: Longitudinal strain and bending stress distributions along cross-sectional element depth at mid-width of ribs 1-3 at different damage states
a, b) damage d1; c, d) damage d4; e, f) damage d5

6. CONCLUSIONS

The reported mechanical behavior of the ribbed wooden element composed of a 3-layer CLT slab and solid wood ribs with significantly different elasticity moduli is representative for this generic type of wood composite. The proven very high capability of load sharing and damage tolerance allows the application of a system strength factor.

Chapter 6 of EC5-1-1 specifies provisions regarding system strength and states that a member strength property may be multiplied by a system strength factor when spaced members, components or assemblies are laterally connected by a continuous load distribution system. In such a case a factor of 1,1 should be applied. In addition for laminated, nailed or glued deck plate systems factors are specified depending on the number of loaded/connected laminations. In case of eight or more laminations k_{sys} values of 1,1 and 1,2 are recommended for nailed and glued assemblies, respectively.

Glued ribbed plates are not explicitly addressed in the provisions for system strength. Based on the available test results it is recommended to introduce a system strength factor of 1,2 for the bending strength of ribs in glued ribbed elements with at least three parallel ribs when manufactured with a CLT slab as sheeting in the compressive zone. Hereby the center distance of the ribs should not exceed the effective width given in EC5 by more than 10% in order to enforce a very pronounced parallel system mechanism.

ACKNOWLEDGEMENTS

The financial support of the reported investigations by Fachagentur Nachwachsende Rohstoffe e.V., Gülzow, Germany, through grant No. 22004014 within the frame of the European ERA-Net+ WoodWisdom project “Hybrid Cross Laminated Timber Plates (HCLTP)” is gratefully acknowledged. The project-involved researchers from MPA University Stuttgart, Department of Timber Constructions, appreciated the fruitful and stimulating co-operation with the scientific partners from

- University of Ljubljana, Faculty for Civil and Geodetic Engineering, Ljubljana, Slovenia
- CBD d.o.o. Contemporary Building Design, Ljubljana, Slovenia
- Vienna University of Technology, Department of Structural Design, Austria

as well as with the industrial partners

- Stora Enso Wood Products GmbH, Brand, Austria and
- Ledinek Engineering d.o.o., Hoce, Slovenia.

Most sincere thanks however are indepted to Dr. Bruno Dujic, CBD, and Dr. Iztok Sustersic (then CBD) for their restless initiation of the project and their utmost friendly leadership.

REFERENCES

[1] ETA-11/0137: *LIGNATUR – box element (LKE), -surface element (LFE) and –shell element (LSE)*. Holder of approval: LIGNATUR AG, Waldstatt, Switzerland, (OIB), Vienna, 2011

[2] ETA-05/0211: *Lignotrend block panel elements*. Holder of approval: LIGNOTREND AG, Gunten, Switzerland. Deutsches Institut für Bautechnik (DIBt), Berlin, 2013

[3] ForestValue_WoodWisdom_Net: *Hybrid cross-laminated Timber Plates (HCLTP)*. Final report (http://forestvalue.org/links/downloads), ForestValue, 2017

[4] N.N.: HCLTP, Final MPA-Report for FNR grant 22004014, MPA University of Stuttgart, 2017

[5] SUSTERSIC, I., DUJIC, B., AICHER, S.: *Less is more – optimized ribbed CLT plates – the future*. New Zealand Timber Design J., Vol. 25 (2), pp. 19 -26

[6] STANIC, A., HUDOBIVNIK, B., BRANK, B.: *Economic-design optimization of cross laminated timber plates with ribs*. Composite Structures, Vol. 154(15), 527-537, 2016

[7] STANIC, A., BRANK, B., KORELC, J.: *On-path following methods for structural failure problems*. Computational Mechanics 57 (1), 1 -26, 2016

[8] DIN 1052-10: *Design of timber structures – Part 10: Additional provisions*. Berlin, Germany: Deutsches Institut für Bautechnik (DIBt), 2012

[9] DIN 4047-1: *Strength grading of wood – Part 1: Coniferous sawn timber*. Berlin, Germany: Deutsches Institut für Normung (DIN), 2013

[10] EN 1912: *Structural timber – Strength classes – Assignment of visual grades and species*. Brussels, Belgium: European Committee for Standardization, 2012 + AC 2013

[11] EN 15425: *Adhesives – One component polyurethane (PUR) for load bearing timber structures – Classification and performance requirements*. Brussels, Belgium: European Committee for Standardization, 2017

[12] DIN EN 1995-1-1/NA: *National Annex – Nationally determined parameters – Eurocode 5: Design of timber structures – Part 1-1: general – Common rules and rules for buildings*. Berlin, Germany: Deutsches Institut für Normung (DIN), 2013

[13] EN 338: *Structural timber – Strength classes*. Brussels, Belgium: European Committee for Standardization, 2016

[14] EN 1995-1-1: *Eurocode 5: Design of timber structures – Part 1-1: general – Common rules and rules for buildings*. Brussels, Belgium: European Committee for Standardization, 2004 + AC:2006 + A1:2008